Digest Journal of Nanomaterials and Biostructures Vol. 10, No. 4, October - December 2015, p. 1229 - 1235

NOVEL NANOSTRUCTURED MOLECULAR SIEVES OF SILICA WITH INCLUDED TITANIUM DIOXIDE: PREPARATION AND CHARACTERISTICS

M. B. M. AL TAMEEMI, D. MIHAIESCU, R. STAN, A. MEGHEA, G. VOICU, B. S. VASILE, V. TRAISTARU, D. ISTRATI*
Facultatea de Chimie Aplicata si Stiinta Materialelor, Universitatea Politehnica din Bucuresti, Romania

In the present work, new nanostructured silica-titanium molecular sieves have been synthesized by a modified sol-gel method, using an acidic solution of titanium as titanium dioxide source, while TEOS have been used as silica precursor. The prepared samples have been characterized by FT-IR, EDAX, XRD, TEM and BET methods. The differences of the surface area values could be correlated with pH levels of the reaction medium and TiO_2 crystallinity. Calcination temperatures affected the transition of titanium oxide, from the (Ti_3O_5) intermediate form, to the final tetragonal titanium dioxide (TiO_2) form.

(Received September 15, 2015; Accepted October 30, 2015)

Keywords: Molecular sieves; Silica-titanium; Sol-gel; Surface area

1. Introduction

Mesoporous materials, also found as mesoporous sieves posses a high pore distribution with a small average pore size. These materials act as catalysts and support materials [1, 2] and they can be combined with larger pore structured materials, in order to obtain better carriers for the catalysts [3-6]. Among materials that have been used as nanostructured sieves, the most relevant ones are nanostructured silica. These materials possess an ordered pore structure and a high surface area, functionalized by silanol groups [7-9]. Silica nano-sieves are used in various industrial domains for paints, cosmetics, catalysis, or for medical purposes as support materials for bone regeneration and drug delivery [9]. These nanostructured sieves have unique physical properties (thermal, optical and electrical) in addition to the biochemical properties such as biocompatibility, non-toxicity and biodegradability [8]. Nanostructured silica materials have generally been prepared by different methods such as: normal pressure precipitation, hydro-thermal precipitation, microemulsion and other methods. Among them, the most efficient method is sol-gel technique, as extensive research demonstrated. The method has two major advantages: it is easy to manage and produces accurate results [9].

The sol-gel method is affected by different factors such as catalysts, solvents, reaction media and other chemical conditions. On the other hand, physical factors such as temperature and the rate of by-products removal also play a significant role. This procedure takes place at low temperature conditions and can be properly controlled, in case other organic or inorganic materials are added to the silica matrix. The addition of those materials can be controlled to the micro- as well as nano-level by encapsulating drugs for control release purposes, or metals for enhanced properties of the silica matrix itself [8].

Some of the challenges of these materials are due to their poor mechanical properties. Moreover, in biomedical applications, when used as drug carriers, silica sieves, such as MCM-41, lead to burst effect, non-sustained and unsteady drug release. These are the main drawbacks using nanostructured silica sieves as drug delivery systems [7] [9]. Adding certain metals to silica

* Corresponding author: d_istrati@yahoo.com

nanostructured materials can improve their structural and mechanical properties and their performance in different applications [10].

Extensive research was conducted using different metals, such as aluminum, cobalt, iron, copper and titanium [6]. The first experimental synthesis of MCM-41 with titanium was around ten years ago [11-14]. The product of this combination is a promising material especially as a catalyst and carrier with interesting biocompatibility and mechanical properties [15]. Moreover, this material has been used in different applications, especially the ones that need a uniform pore structure and extremely high surface area and therefore more active sites [14]. Besides titanium, aluminum is also used for this purpose. However, titanium has less electronegativity in the framework of mesoporous silica, a fact which may adjust the negative charge of the silica surface and therefore provides moderate carrier properties [15]. The most efficient metals are aluminum and titanium, however; the latter is superior due to its excellent biocompatibility and bioactivity. Moreover, titanium has proved successful in practice for various biomedical applications, such as orthopedic implants and dental applications in addition to drug delivery systems [16-18] [10]. Titanium dioxide is known as a material with appropriate biocompatibility with high corrosion resistance [15], good chemical and thermal stability [8]. For this reason, titanium composites are considered some of the most interesting materials in dental and biomedical fields [15]. Furthermore, modifying the mesoporous silica material with titanium dioxide can improve the geometry of the mesoporous structure by changing the straightness and flatness of their channels. The inclusion of titanium dioxide within the silica mesoporous matrix yielded a rough channel structure, this property can be used in controlled release applications to enhance the release period [10].

In the present study, six different samples of molecular nanostructured sieves have been prepared using a sol-gel method, and different experimental conditions. The final materials contain intercalated TiO_2 within the silica matrix. The porosity and surface area of these sieves have been tuned by controlling the solution's alkalinity. Several analyses were carried out for the obtained samples in order to examine their content and characteristics.

2. Experimental

2.1 Materials and characterization methods

TEOS (tetraethyl orthosilicate), CTAB (cetyltrimethylammonium bromide), titanium, sulfuric acid, ethanol, ammonium aqueous solution and ammonium fluoride were purchased from Sigma-Aldrich and used as received from the source, water used in all experiments was ultrapure water type 2 (~15MΩ) obtained from a Millipore Elix5 device.

FT-IR spectra were recorded using Nicolet IS 50 Thermo Scientific double source system with interchangeable beam splitter for near, mid and far domain. The sample introduction system was a single reflexion diamond ATR using FAR-IR domain (1800-100 cm^{-1}) and an average of 32 spectra per scan at 4 cm^{-1} spectral resolution.

X-ray analysis were performed with X-ray powder diffraction patterns using a Shimadzu XRD 6000 diffractometer, using Cu Kα (1.5406 Å) at 30 mA and 40 kV. The 2θ range was 10–80° and the scan rate 1° min^{-1}.

Brunauer–Emmett–Teller (BET) analysis was carried out on a Micrometrics Gemini V2 model 2380. The adsorption isotherms were obtained by measuring the quantity of the adsorbed gas at a wide range of relative pressures with constant temperature (N_2, 77 K and pressure between 780 and 7.8 mmHg). Desorption isotherms were obtained by measuring the gas desorption rate at pressure reduction.

The transmission electron microscopy images were obtained using powdered samples by a Tecnai™ G^2 F30 S-TWIN high resolution transmission electron microscope from FEI, EDS equipped (energy dispersive X-ray analysis), operated at an acceleration voltage of 300 kV obtained from a Schottky field emitter, with a TEM point resolution of 2 Å and line resolution of 1.02 Å.

2.2 Synthesis of silica-titanium sieves

Silica-titanium sieves were prepared by one-pot procedure at room temperature and normal pressure, employing different amounts of ammonium hydroxide (10 mL, 7 mL, 5 mL, 15mL, 2.5 mL). The silica precursor solution contained 7.6 mL (7.09 g) TEOS in 11 mL methanol. Another solution representing the surfactant solution have been prepared by dissolving 0.5 g of CTAB in 18 mL methanol - water mixture (11/7mL) and 0.3g of ammonium fluoride catalyst solution, followed by adding the necessary quantities of ammonium hydroxide. Separately, a stock solution of titanium dioxide was prepared by mixing 5 g of powdered metallic titanium with 50 mL sulfuric acid, followed by stirring for 3 hours while heating at 100 ◦C. Different amounts (1.9 g, 2.7 g) from the titanium solution were used after dissolution in 11 mL of methanol and 10 mL water. The final mixture was prepared by adding the surfactant solution to the precursor solution and stirring at 400 rpm overnight at room temperature. The prepared samples were filtered then washed with excess amount of alcohol and water. A thermal treatment was applied to all samples, at 550 ◦C/ 4 hours and 600 ◦C, 650 ◦C/ 6 hours, in order to establish the best calcination conditions.

3. Results and discussions

3.1 Synthesis of silica titanium sieves

The nanostructured sieves have been prepared according to sol-gel principle, however, the addition of the Ti acidic solution in the gelation step, as an accessible titanium oxide precursor, yields a more convenient way for the synthesis of titanium-silica composites. The formation of silica titanium sieves, using TEOS as silica source, in the presence of CTAB as surfactant, leads spherical nanoparticles with about 150 nm diameter. The purpose of titanium addition during gelation phase is related to titanium oxide chains intercalation in the silica matrix with an expected pore size modification. The influence of the pH on silica hydrolysis and certainly on the porosity properties was studied by the variation of the base amount (ammonium hydroxide). The distribution of the titanium oxide in the silica matrix can be correlated with the differences of the surface area values and the specific reaction conditions. The molar ratios of titanium dioxide, ammonium hydroxide and silica, used in different experimental stages, are listed in Table 1.

Table 1 - The molar ratios of TiO_2 with NH_4OH and SiO_2

Sample	TiO_2/ NH_4OH (Moles/ Moles)	TiO_2/ SiO_2 (Moles/ Moles)
1	1.9/ 13.5	1/ 8.5
2	1.9/ 9	1/ 8.5
3	1.9/ 6.3	1/ 8.5
4	1.9/ 4.5	1/ 8.5
5	1.9/ 2.25	1/ 8.5
6	2.7/ 2.25	1/ 6

3.2. Sample characterization

FT-IR spectra for silica-titanium sieves, Fig. 1, shows a broad band at 1064.4 cm^{-1} that refers to the asymmetric Si-O stretching modes, also a small band at 800 cm^{-1} was associated with the symmetric stretching modes of Si-O bonds [6]. A broad band at 444.4 cm^{-1} was correlated with the presence of the TiO_2 structure [19].

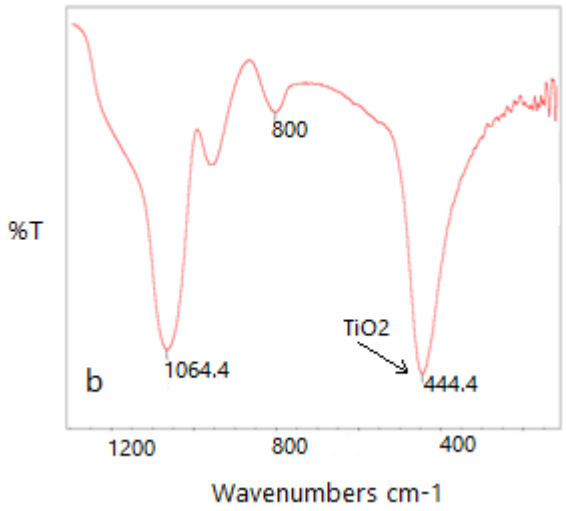

Fig. 1 FT-IR spectrum of silica-titanium sieves

The elemental composition of the dried samples was examined by EDAX analysis proving Si, Ti an O presence, the Ti peak intensity can be correlated with the titanium / silica ratio (1/ 8.5) Fig. 2a, and a higher titanium ratio (1/ 6) Fig. 2b.

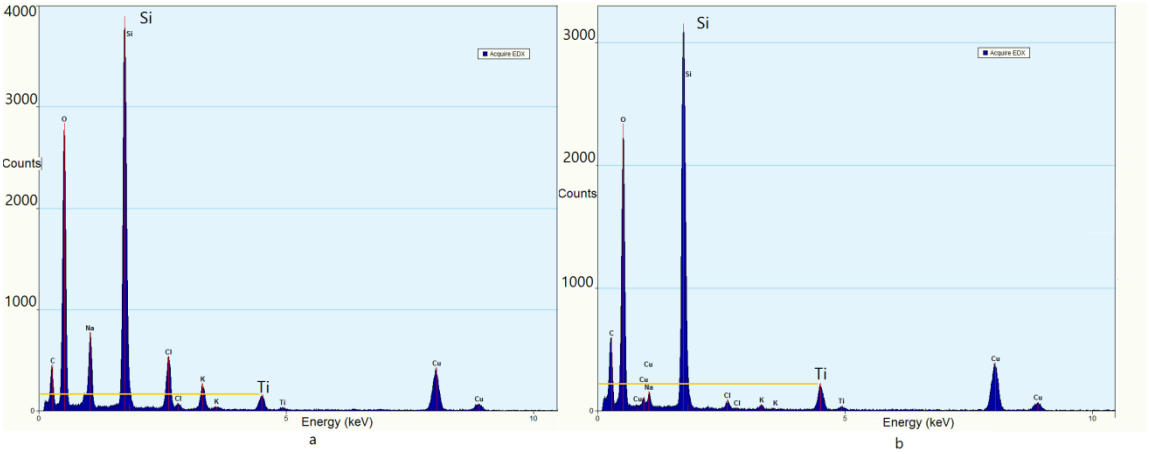

Fig. 2 (a): EDAX analysis of the samples with ratio of (1/ 8.5) TiO_2/ SiO_2. (b): ratio of (1/ 6) TiO_2/ SiO_2.

A thermal treatment study were performed using sample 5, in order to establish the best calcination temperature related to the anatase phase transition. The XRD patterns were obtained for sample 5 after thermal treatment from 500°C to 650°C. After thermal treatment at 500°C/4h, the specific signals of SiO_2 (JCPDS 83-1832) are observed accompanied by specific signals of an intermediate form of titanium oxide (Ti_3O_5, JCPDS 72-2101). By increasing the temperature and thermal treatment plateau, progressive formation of TiO_2 anatase occurs, subsequently to the disappearance of the intermediate form of titanium oxide [20][21]. Also, at the 650°C/6h a low crystallinity degree in accordance to TEM results and the specific signals of TiO_2 anatase (JCPDS 84-1286) and SiO_2 (JCPDS 83-1832) are observed.

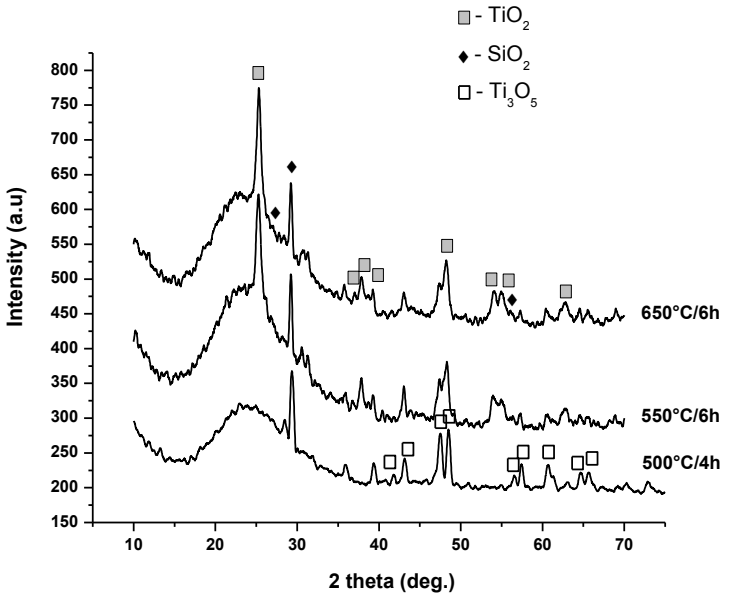

Fig. 3 XRD patterns of Silica-Titanium sieves prove the influence of the calcination temperature in the transition from the Ti intermediate state to the final anatase phase

TEM photos Fig. 4a show that spherical nanoparticles have been produced with an average diameter around 150 nm. However, the image with 2 nm drawing scale (Fig. 4b) shows a distribution of the titanium oxide crystalline regions in the silica matrix, for the sample obtained under highest pH levels (anatase titanium oxide crystalline phase can be distinguished from the surrounding silicon oxide amorphous phase).

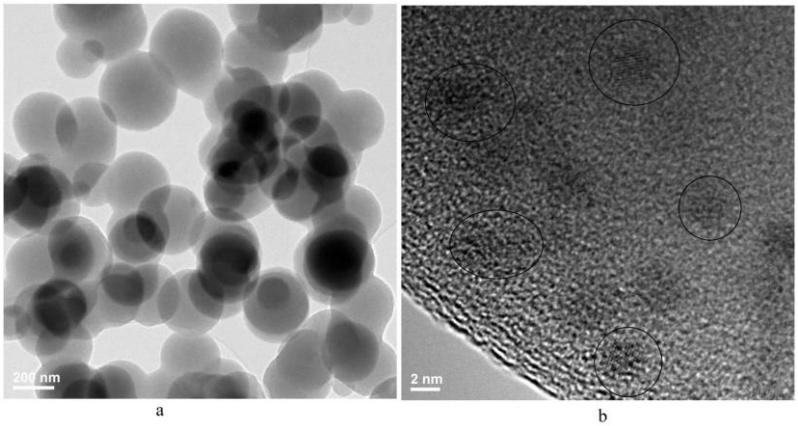

Fig. 4 (a): TEM photo shows the spherical shape of the final nanoparticles. (b): the crystallinity spots of the sample prepared under most alkaline conditions

The pore diameter and surface area have been measured by using BET analysis and all samples show close pore size - about 3.03-3.9 nm average diameter. The surface areas showed significant different results: the lowest surface area was around 84 m^2/g, whereas the highest surface area was 528, Table 2, these results can be correlated with the different experimental conditions and pH differences, but also with the presence of TiO_2 anatase phase (the presence of amorphous TiO_2 phase is correlated with highest surface area values).

Table 2 - The relation between the pH value, surface area and pore sizes

Sample	pH	BET Surface area m^2/g	Average pore diameter (4V/A)
1	10.1	179.5177	3.9837 nm
2	8.8	221.1669	3.4160 nm
3	7.2	83.9210	3.8691 nm
4	5.0	175.4848	3.3791 nm
5	2.6	528.4277	3.7756 nm
6	-	331.0430	3.0329 nm

The small differences of pore size diameter can be correlated with the similar mechanism involved in silica structure formation, and the low CTAB concentrations used for all experiments, significantly lower than the concentrations used for the synthesis of MCM41 - type materials with mezoporous structure and high pore diameter structure. However, the significant difference in surface areas can be correlated with the pH differences at the gelation step, the presence of the anatase crystallinity phase and the nanoparticle diameter. A possible explanation of the surface area distribution can be linked to the differences between the reaction rates of the precursor species. The hydrolysis rate of TEOS is high under alkaline-, low under neutral- and average under acidic-conditions. On the other side, the titanium precursor shows an average reaction rate in acidic medium with significant increase in neutral and alkaline conditions. The formation of TiO_2 anatase inclusions in the SiO_2 matrix would dramatically decrease the surface area. Our supposition sustained by the observed TEM images (Fig 4.b.) is related to the correlation of a higher segregation at low TEOS / high titanium precursor reaction rates (highest observed TiO_2 crystallinity spots) with low surface area, under neutral condition [22] [23]. Under acidic conditions an average reaction rate for both precursors yields an intercalation of Ti-O in the Si-O chains and no observed crystallinity in the TEM image, correlated with highest observed surface area. Using alkaline conditions at a high reaction rate for both precursors, TiO_2 crystallinity decreases (yielding higher surface area, but significantly lower than under the acidic conditions). The reason behind that is related to the lower time of the titanium precursor to produce crystalline areas.

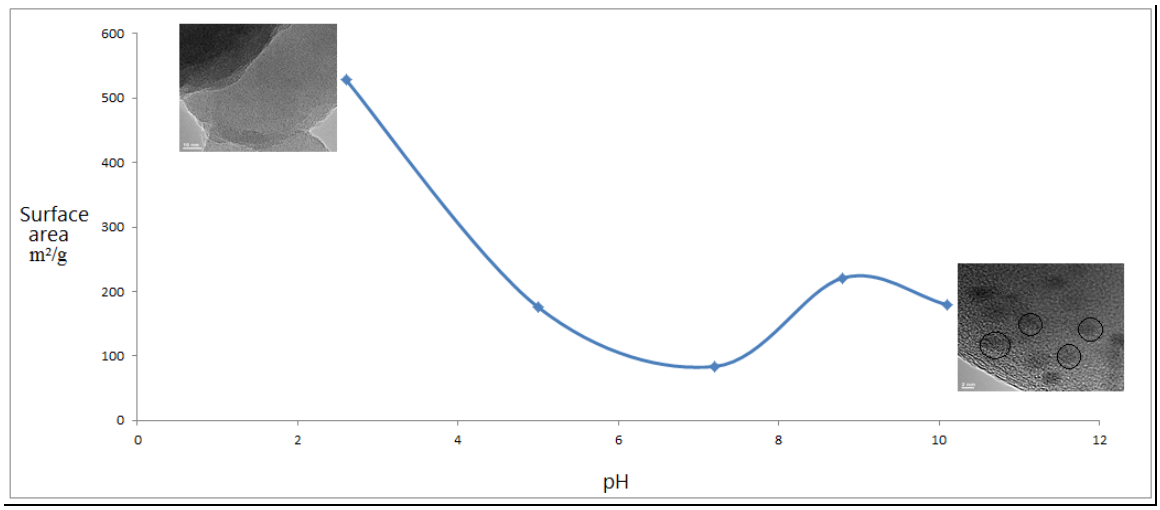

Fig. 5 Diagram illustrates the relation between the pH value and surface area. The correlation with crystallinity level proves higher crystallinity at higher pH levels

4. Conclusions

Silica-titanium sieves, with spherical nanostructured shape were successfully prepared in different chemical conditions, with various surface areas and TiO_2 crystallinity levels. The influence of the calcination temperature in the anatase phase formation and of the pH level in the final surface area was studied. Values over 500 m^2/g were obtained for the spherical nanoparticles with 150 nm average diameter, and the best experimental conditions for higher surface areas were established. Higher levels of TiO_2 involving higher anatase phase segregation after the calcination step yield to lower surface areas. The highest surface areas are related to a better intercalation of titanium in the silica structure, with lower observed crystalinity. Both types of materials can be good candidates for drug delivery supports in controlled release experiments, with enhanced biocompatibility related to the titanium content, but also for other applications as biocompatible thin films, sensors, solar cells and other advanced applications.

Acknowledgments

The contribution of Vanessa Traistaru has been funded by the Sectoral Operational Programme Human Resources Development 2007-2013 of the Ministry of European Funds through the Financial Agreement POSDRU/159/1.5/S/134398.

References

[1] P. Selvam, S.K. Bhatia, C.G. Sonwane, Ind. Eng. Chem. Res. **40**, 3237 (2001).
[2] C.T. Kresge, M.E. Leonowicz, W.J. Roth, J.C. Vartuli, J.S. Beck, Nature **359**, 710 (1992).
[3] O.A. Anunziata, M.L. Martínez, M.G. Costa, Mater. Lett. **64,** 545 (2010).
[4] F.S. Xiao, Y. Han, Y. Yu, X.J. Meng, M. Yang, S. Wu, J. Am. Chem. Soc. **124**, 888 (2006).
[5] M.M.L. Ribeiro Carrott, F.L. Conceicâo, J.M. Lopes, P.J.M. Carrott, C. Bernardes, J.Rocha, F. Ramôa Ribeiro, Microporous Mesoporous Mater. **92**, 270 (2006).
[6] Dewen H., Cancheng B., Chongwen J., Tao Z., Powder Technology **249**, 151 (2013).
[7] B. Allo, A. Rizkalla, K. Mequanint, ACS Appl. Mater. Interfaces **4**, 3148 (2012).
[8] Z. Jianling, L. Zhimin, H. Buxing, L. Zhonghao, Y. Guanying, L. Junchun, C. Jing, J. of Supercritical Fluids **36**, 194 (2006).
[9] M. Catauro, F. Bollino, F. Papale, Arabian Journal of Chemistry **2015**, 1 (2015).
[10] M. M. Wan, X. D. Sun , S. Liu , J. Maa,, J. H. Zhu, Microporous and Mesoporous Materials **199**, 40 (2014).
[11] T. Blasco, A. Corma, M.T. Navarro, J.P. Pariente, J. Catal. **156**, 65 (1995).
[12] P.T. Tanev, T. Chibwe, J. Pinnavaia, Nature **368**, 321 (1994).
[13] A. Corma, M.T. Navarro, J.P. Pariente, J. Chem. Soc. Chem. Commun. (1994) 147.
[14] C. Galacho, M.M.L. Ribeiro Carrott, P.J.M. Carrott, Microporous and Mesoporous Materials **100**, 312 (2007).
[15] J. Pan, C. Leygraf, D. Thierry, A. M. Ektessabi, Journal of Biomedical Materials Research **35**, 309 (1997).
[16] D. Buser, U.C. Belser, L.N. Pang, Periodontology **17**, 106 (2000).
[17] M.Z. Zhao, Q.S. Wang, W.J. Lai, X.Y. Zhao, H.Y. Shen, F.L. Nie, Y.F. Zheng, S.C. Wei, J.G. Ji, J. Mater. Chem. B **1**, 1926 (2013).
[18] W.T. Peng, Z.M. Qiao, Q. Zhang, X.D. Cao, X.F. Chen, H. Dong, J.W. Liao, C.Y. Ning, J. Mater. Chem. B **1**, 3506 (2013).
[19] M. Grujic-Brojcin, M. J. Scepanovic, Z. D. Dohcevic-Mitrovic, I. Hinic, B Matovic, G. Stanisic, Z. V. Popovic, J. Phys. D: Appl. Phys. **38,** 1415 (2005).
[20] Z. Zhang, B. Gu, W. Zhu, L. Zhu, Experimental and therapeutic medicine **6**, 707 (2013).
[21] Y. Lee, M. Kang, Materials Chemistry and Physics **122**, 284 (2010).
[22] M. Buckley, M. Greenblatt, Journal of Chemical Education **71**, 599 (1994).
[23] L. L. Hench , J. K. West, Chem. Rev. **90**, 33 (1990).